Applications of Abaqus/Explicit to Flexible Packaging

Shiming Zhuang

Bemis Company, Inc.

Abstract*: This paper showcases the applications of Abaqus/Explicit to the R&D of flexible plastic packaging films and products that Bemis Company is currently engaging to, particularly in the areas of liquid pouch packaging and thermoforming of medical device packages. The pouch burst strength was analyzed using the shell element with fluid cavity technique and it was found that the material ductility affected the pouch failure modes or locations. The pouch liquid filling and drop impact performance was modeled with the smoothed particle hydrodynamics (SPH) method, which revealed that upon impact from a drop height of 4 to 5 feet the deformation rate in the pouch was on the level of or over a hundred per second. For simulation of thermoforming of syringe packages the shell element and fluid cavity were used with super-elasticity material models to predict wall thickness distribution. Bemis Company is one of leading global companies delivering customers flexible and rigid plastic packaging of food, consumer goods, medical devices and pharmaceutical products.*

Keywords*: Abaqus/Explicit, Fluid Cavity, SPH, Flexible Packaging, Pouch Air Inflation, Pouch Burst Strength, Pouch Liquid Filling, Pouch Drop Impact, Thermoforming, Medical Device Packaging.*

1. Introduction

Plastic packaging is a fast growing business with a global market value over US$310 billion in 2017. The flexible plastic packaging shares one third of the market and grows at a compound annual growth rate (CAGR) of 5.2%, projected to reach a market value over US$130 billion by 2022[1]. Bemis is one of major global suppliers in flexible and rigid plastic packaging for food, consumer products, medical and pharmaceutical companies, serving its customers with a wide range of products including pouches, bags, wraps, trays, roll-stock films while providing customized packaging design, technology and process innovative solutions[2].

Pouch air burst test is a simple yet widely used method in pouch design to evaluate their strength performance. Liquid pouch drop test is another widely used method to assess failure resistance of pouch subjected to the drop impact, which is critical to prevent the pouch from failure in the shipment and potential consumer mishandling (drop). Thermoforming is a manufacturing process widely used in the plastic packaging. The most challenging problem probably should be how to produce parts having a uniform, or a desired, wall thickness distribution. Numerical modeling is found to be an extremely useful tool for the forming process setting and material development.

In 2017 Bemis introduced Abaqus program, aimed to develop numerical modeling applications to the research and development of packaging materials, manufacturing process improvement and customer supports for packaging design and product performance assessment. Grateful to the support from Bemis management and R&D teams, and the Abaqus technical support, exciting progress has been made in use of the program to the interest topics. Three application cases presented here are: pouch air inflation and bursting, pouch liquid filling and dropping, and thermoforming of medical device packages.

2. Modeling of pouch air inflation

There are a variety of ways to make pouches. A stand-up pouch can be made with three pieces of film. In between the two identical films, with the sealant surface facing each other, sandwiched a gusset piece that is symmetrically folded in the way that the sealant surface is in contact with the two large film pieces (Figure 1). The pouch is usually pre-sealed along two side and bottom edges, leaving the top open for filling. The top open is closed or sealed once the filling is down to finish the packaging. Pouch volume filling limit (volume capacity) and strength performance (service liability) are the two of the most concerns in the pouch design. They are customarily determined iteratively in lab through the filling test and the air burst test, which are both time and labor consuming. We will see soon that the two design parameters/tests can be addressed easily and more economically using a single numerical model.

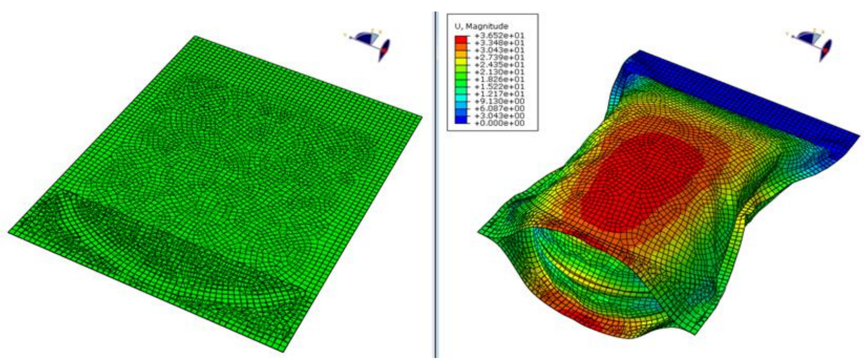

Figure 1 A stand-up pouch made of three film pieces (top, gusset and bottom) expands outwards to increase its volume upon inflation with pressurized air.

The surface-based fluid cavity technique [3] was used to model the air inflation of pouches with Abaqus/Explicit. The film was meshed with the conventional shell element (S4R). Usually, the default value of mesh size was taken while a finer mesh was used sometimes. The tie constraint was applied to all of the pouch seals. Typically, pouch films are of multilayer configuration, consisting of sealant, outer, barrier and other layers. For simplicity, the film was treated as an isotropic homogenous elastic-plastic material with a linear strain hardening behavior, failed at some ultimate stress or strain. In the Abaqus fluid cavity, the exerting of fluid force is realized by treating all the surfaces of the cavity as interior boundaries, on which a pressure is applied through an analytical function of time. In this modeling, a linear (or stepwise) increase of the cavity pressure with time was used to simulate the air inflation of pouches. The volume capacity of the pouches in concern was in the range of 3 to 16 ounces (oz.).

2.1 Sizing of pouch filling volume

Figure 2 shows the curves of pouch interior surface pressure (exerted boundary condition), pouch volume and the total plastic dissipation energy as a function of time. It is seen that the pouch volume increases with air pressure, which can be characterized into three ranges. Range I corresponds to the period of volume increase that all the film elements deform elastically, i.e., zero-plastic energy dissipation. This is the period that the pouch volume increasing is the fastest. In range II, the volume increase is slowed down while the plastic dissipation increase quickly and nearly linearly. In range III, the increases in both pouch volume and the plastic energy are flattened out. In fact, the range II corresponds to the yielding of elements in the zones where stress concentration happens the earliest, such as the triple areas. Consecutively, the range III represents the localization of plastic flowing in those zones, and/or growing into the new zones.

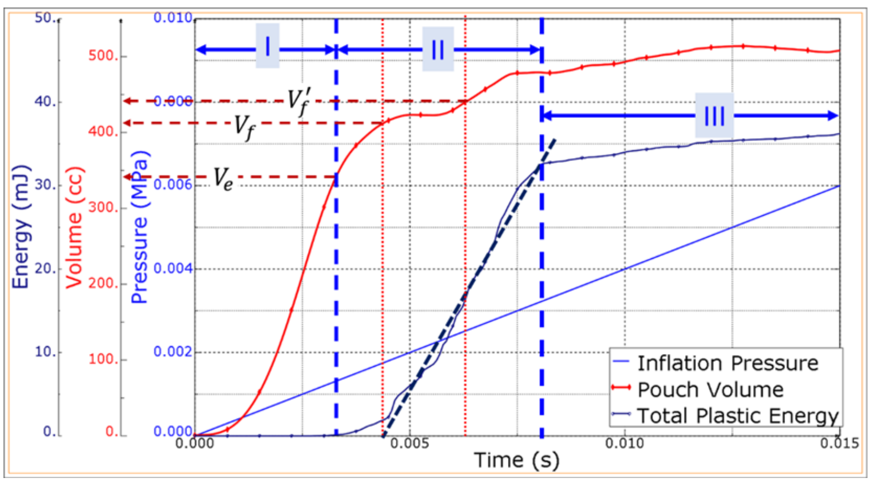

Figure 2 Pouch interior pressure, volume and total plastic dissipation energy as a function of time.

In practice, pouches are always subjected to some level of loading, and they are very tolerable to some degree of yielding without failing their designed functions due to the nature of ductile polymer materials being able to carry force to a very large deformation state. It is noticed that the amount of the plastic work in the range II is actually on a quite low level. Let us define the middle point of the range II being the plastic dissipation limit allowed, and denote it as V_f'. Similarly, define V_f as the pouch volume at the nominal zero-plastic work point, the intercept of the straight line approximating the linear increase in plastic work in the range II (Figure 2), V_e the pouch volume at the right boarder of the range I, i.e., the elastic limit volume.

Table 1 summarizes the modeling results of V_e, V_f, and V_f' volumes for 5 pouch designs. The pouch samples of the 5 designs were made for filling test to measure the filling volume V_{test}. The measured results are also listed in Table 1. It is seen that setting either V_f' or V_f as the pouch volume filling limit is quite reasonable. It is recommended that using the modeling determined V_f' as the reference of volume limit set the pouch volume filling capacity as $(0.85 - 0.95)V_f'$, which gives a 5-15% headspace.

Table 1 Comparison of pouch volumes by modeling and filling test

Pouch Filling Volume Capacity Study					
Case #	Base	#1	#2	#3	#4
V_{target} (oz.)	14	16	16	16	16
V_e (cc)	250	235	260	270	170
V_f (cc/oz.)	410 (14.4)	365 (12.9)	410 (14.4)	420 (14.8)	360 (12.7)
V_f' (cc/oz.)	455 (16.0)	435 (15.3)	470 (16.6)	500 (17.6)	400 (14.1)
V_{test} (cc/oz.)	397 (14.0)	/	468 (16.5)	478 (16.9)	350 (12.3)

2.2 Burst strength of pouches

In modeling of pouch air inflation, if increasing the cavity pressure further, the pouch will continuously expand to a larger and larger volume, in which more and more elements will become yielding, then flowing plastically. The pouch will eventually burst when the element with the largest plastic strain reaches the break limit. Figure 3 shows a stress-strain curve of typical pouch film materials. The material can deform to a quite large strain with a middle level of strain hardening and breaks at 80% and 90% of engineering strain for stretching along MD and CD, respectively.

To simulate pouch burst test, a material progressive damage based failure model was used. The forming limit stress diagram (FLSD) damage initiation criterion and the linear damage evolution based on effective plastic displacement were selected. Once the value of specified maximum effective plastic displacement is met, an element is failed and removed from the mesh.

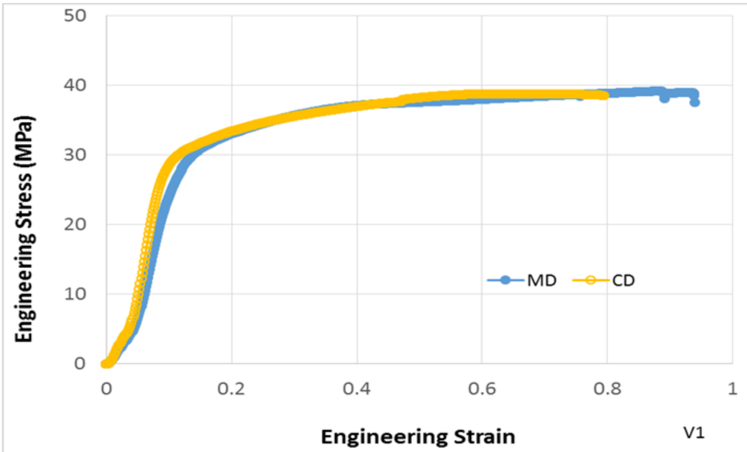

Figure 3 Typical stress-strain curve of flexible packaging films

Six pouches, of different volume filling capacities, designs (geometrical dimensions), film materials and seal methods, were made and air-burst tested. Their burst pressures are listed in Table 2. The burst samples were examined to determine their failure mode/location, together with the results obtained by the numerical modeling analysis of the tests are listed in the Table 2.

Table 2 Comparison of pouch burst pressures by burst test and Abaqus modeling

Sample ID	Volume Size	Design ID	Film Mat.	Making Method	Burst test	FEA Modeling	
					Failure pressure	Failure location	Failure pressure
	(oz.)				(psi)		(psi)
V1	4.0	D-1	F-1	Manual	16.18	Triple	23.34
V2	3.5	D-2	F-1	Manual	19.08	Triple	28.64
V3	4.0	D-1	F-2	Manual	16.04	Triple	22.60
V4	3.5	D-2	F-2	Manual	19.19	Triple	23.71
V5	4.0	D-1	F-3	Machine	23.46	Belly	23.06
V6	3.2	D-3	F-3	Machine	26.17	Triple	30.71

It is seen from Table 2 that in general the modeling trends to over predict the burst pressure, especially for the cases of manually made pouches. The reason may be due to the thickness reduction (or partial damage) in the film in the sealed areas and their neighboring since the pouches were thermally sealed under pressure. This thickness reduction (or the possible weakening) was not taken into account in the modeling analysis. It became worse for the handmade pouch cases, if a higher seal pressure was applied or the pressure was not evenly imposed across seal areas, resulting in the pouch to fail at an even lower air pressure in the burst test.

The detail and accuracy of film material failure was not pursued in this early stage of Abaqus application development, so a pouch was allowed to fail simply once the break stress was reached. To achieve it in the failure model selected, the value of maximum plastic displacement was set to 0.1 to 0.2 times of the average element size. Under this failure criterion, the pouch damaged and failed most likely around the triple point, and then propagated along the edge of the side seal and the middle of the gusset as shown in Figure 4, which was the failure mode most often observed in the burst tests (Table 2).

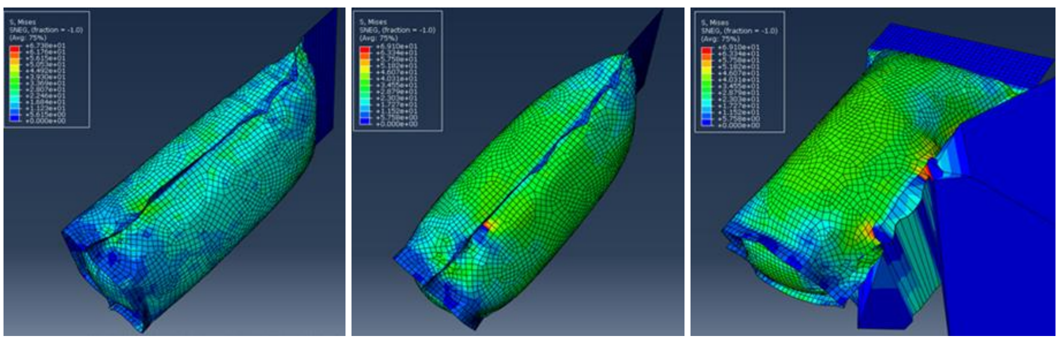

Figure 4 Air inflation and burst of pouches with elastic-plastic film and progressive damage to failure around the triple point under the small effective plastic displacement of one tenth of the element size.

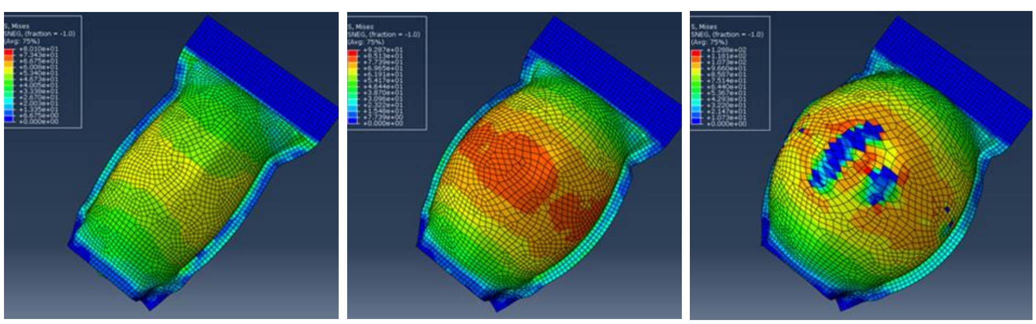

Figure 5 Air inflation and burst of pouches with elastic-plastic film and progressive damage to failure at “belly” area under the large effective plastic displacement of 10 times of the element size.

To explore the effect of film material ductility on the pouch burst failure, we changed the damage initiation criterion from the FLSD to the forming limit diagram (FLD) and increased the damage initiation plastic strain value 70% higher than that corresponding to the damage initiation stress specified in the FLSD (more ductile). The damage evolution law and the failure plastic displacement were kept be the same. The modeling result indicated that instead of the damage initiated around the triple points, the pouch expanded further to a much larger volume as seen in Figure 5, looking like a balloon. The damage initiated at the center, i.e., the "belly" area, and eventually the failure occurred there, which was also observed in the burst test (Table 2).

3. Modeling of pouch liquid filling and drop impact

The modeling analysis of liquid pouch drop impact performance consists of two models. The first is built above the air inflation model described in the previous section, including construction of a flat pouch (Figure 6a), inflating it slightly (Figure 6b), following by an additional step to open two slots (Figure 6c), one for filling liquid and the other for installing a fitment. In the second model, the deformed pouch parts were imported from the outputs of the first model, then a solid column representing the liquid (water) with the desired mass was added (Figure 6d). For the drop impact, a rigid floor was assembled at a desired distance from the pouch (Figure 6f), and to assist the close of the filling slot after the liquid filling a pair of rigid flat plates (Figure 6e) were installed to push the pouch top seals toward each other. In brief, this analysis includes three steps, liquid filling (Figure 6d), closing the filling slot (Figure 6e), and drop to impact onto the floor (Figure 6f and 6g).

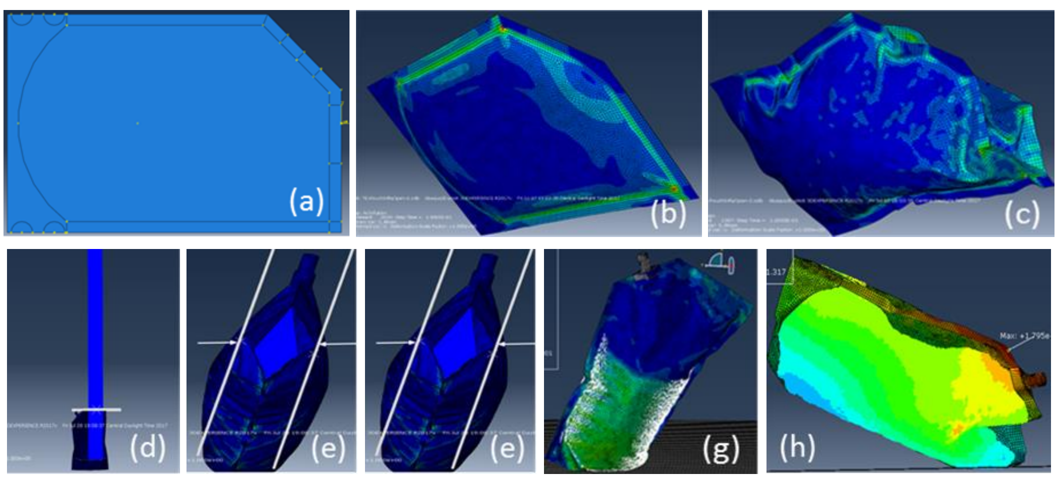

Figure 6 Numerical modeling of pouch liquid filling and drop impact

The smoothed particle hydrodynamics (SPH) numerical analysis technique [3] was used to model the liquid flowing and interaction with pouch walls. The liquid column is initially created as a solid part, meshed with 3D solid elements which are allowed to be converted into SPH particles at the begging of the analysis. Desired fluid properties are assigned to the SPH particles. Pouch film is modeled the same way as in the modeling of pouch air inflation, using shell elements, elastic-plastic material response and progressive damage leading to failure. The fitment is modeled as a deformable elastic solid, which will do if treating it as an analytical rigid part. Others are modeled as analytical rigid parts. In closing of the liquid filling slot, separation is not allowed once the film interior/sealant surfaces are in contact, which is treated differently from the surface interaction between the pouch film-push plate surfaces where contact and re-separation is conditionally allowed.

Figure 6g shows the stress contour in the pouch surface at about 20 millisecond after impacting onto the floor for the case of 4 feet drop with a landing orientation angle (pouch bottom surface with respect to the floor surface) of about 20 degree. The primary deformation (plastic wave in the film and reflection wave in the liquid) front is at the middle of the pouch in propagating from the pouch bottom to the top. The interactions of the pouch with the floor and the liquid with the pouch walls causes the pouch bouncing back up, rotating and then relanding due to gravity.

Figure 6h shows the velocity contours in the fluid and in the films of the back and gusset pieces at about 200 millisecond, at the moment when the pouch is relanding after bouncing up with a top corner touching the floor first. The contour has a center nearby the pouch bottom corner that first impacted onto the floor, which is the rotation center of floor particles. The farther away a particle from the center, the larger its velocity. The particles moving the farthest are to impact onto the fitment and then reflect back, so the sloshing of fluid around the fitment can be seen clearly. The slosh will cause high stresses built up in the film around the fitment. It is especially risky to fail the fitment-film seal around the triple point if stress level becomes high over the area. No surprise, the modeling indeed shows that the stress peaks are likely to be developed nearby the fitment, around the triple point (Figure 7 left), the middle or along the edge.

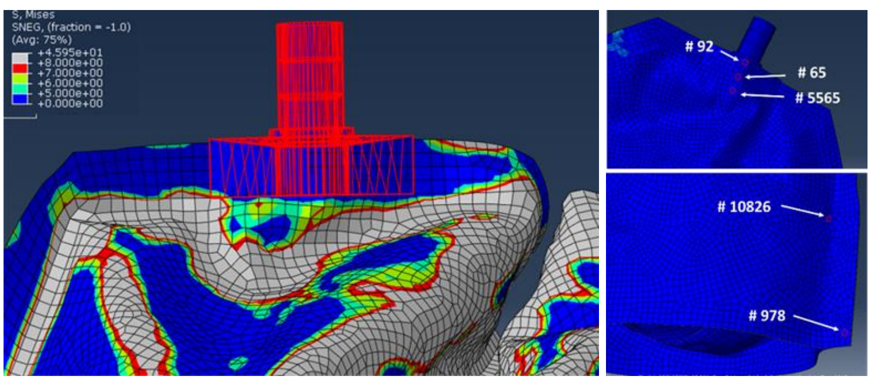

Figure 7 Mises stress contour in film around the fitment – 4 feet drop (left) and element locations for stress history output (right). Right-top: fitment elements #5565, #65 and #92; Right-bottom: triple element # 10826 and corner element # 978.

History outputs of selected fitment elements and triple point elements (Figure 7 right) were made and the stress-time curves of the fitment and the triple point elements are shown in Figure 8a and 8b, respectively, for two drop heights of 4 and 5 feet. In general, stresses at the triple point where experiences the highest stress concentration are about one order higher than that nearby the fitment in the assumed drop orientation. Two jumps can be seen from the triple point stress curve. The first is a slower increase corresponding to the liquid filling. The second is rather sudden in a time scale of 2-5 millisecond due to impact onto the floor, which resulted in a plastic strain on order of 0.2 to 0.3. So, the plastic deformation in the drop event can be as high as $10^2 s^{-1}$.

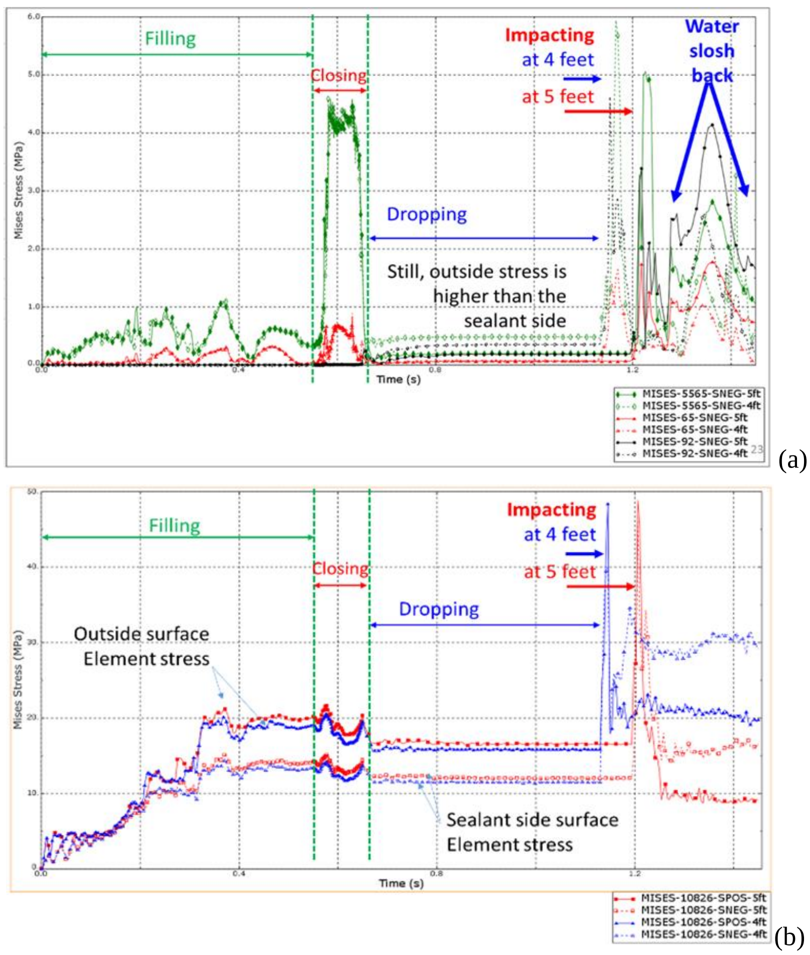

Figure 8 Stress-time curves of fitment elements (a) and the triple point element (b). SNEG=stress at the negative surface side, the sealant surface, SPOS=stress at the positive surface side, the outer surface.

Figure 8a shows that the stress histories of elements along the fitment axis are quite different. For instance, the filling slot closing induced stress is over 4MPa for the element at the inside edge of the fitment (#5566) while it is nearly zero for the element located at the outer edge of the fitment. The stress peaks induced by liquid sloshing is clearly observable. At the specific location of selected element #5566, the stress is about 1.5 MPa and 3MPa for 4 feet and 5 feet drop. For the 4 feet drop, the highest stress is found near the triple seal of the fitment with an amplitude close to 10MPa (Figure 7 left).

4. Modeling of thermoforming products and strength prediction

Modeling of thermoforming syringe packages is conducted using ABAQUS/Explicit with the fluid cavity technique. The mold is modeled with rigid surface shell element. The film is modeled with deformable 3D shell element. Hyper-elasticity material model, Yeoh model, is used to describe the film deformation behavior at the thermoforming temperatures. The flat film sheet is initially set at the top of the surface (not shown in Figure 9a). A negative pressure (vacuum) is applied to the interior surfaces of the cavity formed between the flat film and the mold.

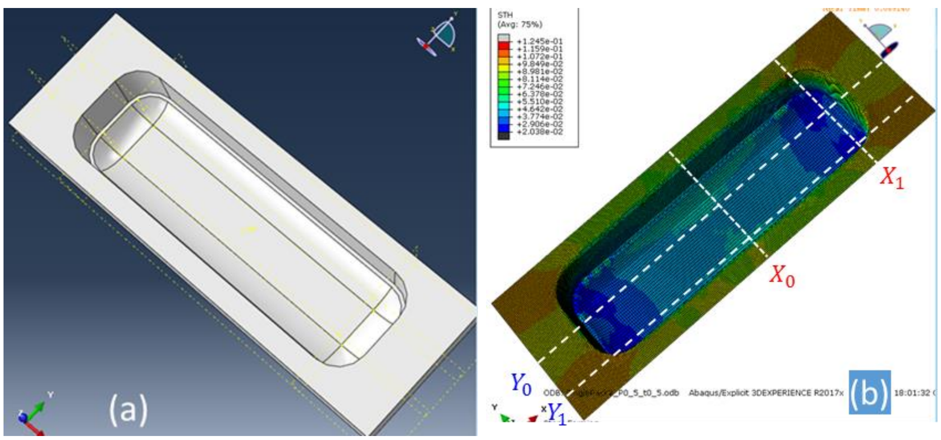

Figure 9 Thermoforming mold modeled with rigid surface shell (a); the wall thickness contour of the thermoformed syringe packet (b). The film initial thickness is 100μm.

A trial was conducted to thermoform syringe package using 100μm thickness film with the mold in Figure 9a. The wall thickness was measured along two central paths X_0 and Y_0 and two edge paths X_1 and Y_1. The wall thickness distributions of thermoforming trial and measurement are compared with that of modeling analysis in the Figure 10. Both the trial and modeling results reveal that the packet wall at the four corners is the thinnest and agree each other quite well. On the other hand, the modeling tends to over-predict the wall thickness in the center areas. It is seen that the distribution curves by the modeling analysis is shifted towards to the right, which is believed to be mainly caused by the factors. The first is the shrinking of the thermoformed package during cooling, resulting in a shorter distance for a given wall thickness point. The second is that the non-penetration restriction was not imposed between the interior surfaces of the film and the mold during the closing of cavity, some degree of over-penetration of the film surface into the mold surface happened, resulting in a longer distance for a given wall thickness. A more sophisticated material model is needed to improve the prediction of numerical modeling analysis.

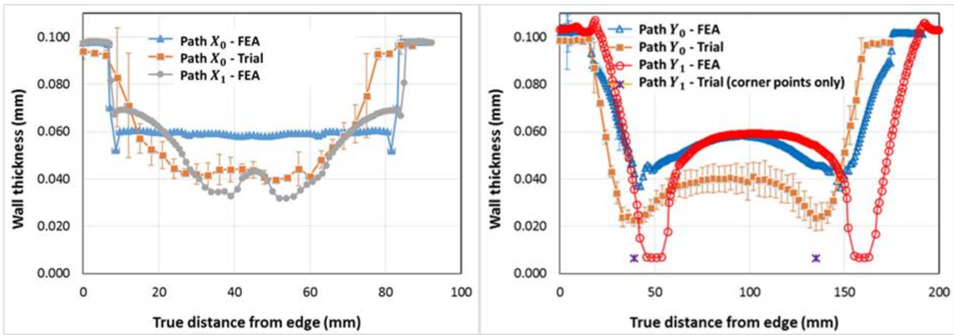

Figure 10 Comparison of wall thickness distributions of modeling analysis results with measurement data of thermoforming trial

To simulate the puncture test of the thermoformed syringe package, a new model is created in which the deformed film part is imported from the first model. A puncture probe is added and assembled to the desired location with a proper orientation (Figure 11). Deformable shell element was used to model the film part and the surface rigid shell to the probe. Elastic-plastic material behavior at the service temperature of the packaging application was assigned to the package wall. The progressive damage fracture model with the FLSD damage initiation and the linear damage evolution was employed to predict the failure of the film. A proper boundary is assigned to the top edge of the package and a displacement boundary is imposed to the top end of the probe for penetration.

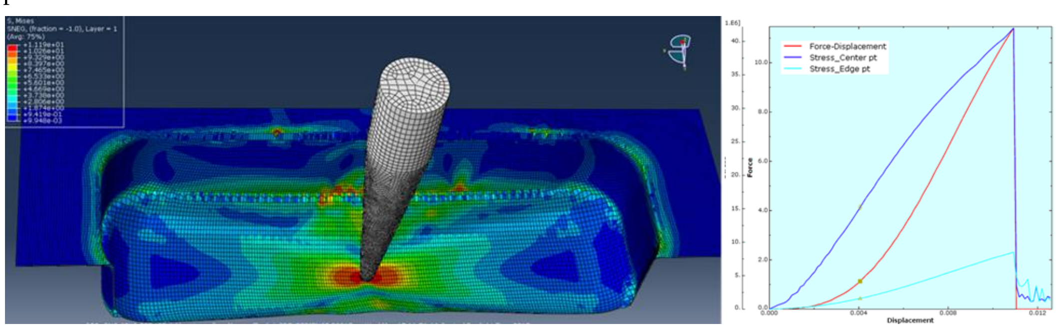

Figure 11 Modeling analysis of a rigid probe puncturing through a thermoformed syringe package. Left: stress contour; Right: force/stress-distance curves.

The total force on the probe end surface (Figure 11, right) reflects the resistance of the package to the puncturing, which accounts for the effect of film layer structuring, component strength, wall thickness uniformity, etc. The combination of the two analysis models will be a useful tool for development of cost-effective packaging films and design of medical device packaging with a desired service performance.

5. Summary and conclusions

The feasibility and benefits of applying Abaqus/Explicit to Bemis' research and development on the flexible plastic packaging materials and products are demonstrated through three modeling examples, the pouch air inflation and burst test simulation, the pouch liquid filling and drop test simulation, and the thermoforming of syringe packages and puncture test simulation.

Two numerical techniques, the surface fluid cavity and the smoothed particle hydrodynamics (SPH), were employed in the developing of the aforementioned numerical analysis models, which makes it easy to model the fluid-solid-interaction (FSI) problems that are otherwise difficult or tedious to be modeled with traditional numerical methods.

Shell type elements are adopted, which fits naturally the feature and properties of flexible packaging materials – multi layer laminated thin sheet configurations.

Our primary focus has been on the identifying of proper numerical methods/techniques and developing them into modeling platforms/tools that will help our R&D the best on the flexible packaging innovations and support our customers on the packaging design and process development.

Though only very preliminary results were obtained with the constructed numerical models, the results are exciting and demonstrated the robustness of Abaqus/Explicit in analysis of flexible packaging related problems.

The future efforts will be on the material property characterization and constitutive model calibration/development to leverage the prediction and application of the developed models, and new numerical model development for new applications.

6. References

1. https://www.marketsandmarkets.com/
2. http://www.bemis.com/
3. Abaqus Analysis User's Guide (2016).

7. Acknowledgements

The author would like to thank the following for their support and help: Chris L Osborn, William E Jackson, Curtis R Barr of Bemis managements; Kurt R Moe and Scott M Kopelke in Bemis IT; special thanks to Romil Tanov, Shyam Kumar, Arun Krishnan, Ramji Kamakoti, Ashwani Goel, Kunming Mao and Yan Xu in the Technical Sales and Technical Support teams of Simulia.